Journal of Power Sources 196 (2011) 860–864

Contents lists available at ScienceDirect

Journal of Power Sources

journal homepage: www.elsevier.com/locate/jpowsour

Short communication

Surfactant-assisted electrochemical deposition of α-cobalt hydroxide for supercapacitors

Ting Zhao [a], Hao Jiang [a,b], Jan Ma [a,b,*]

[a] School of Materials Science and Engineering, Nanyang Technological University, Singapore 639798, Singapore
[b] Temasek Laboratories, Nanyang Technological University, Singapore 637553, Singapore

ARTICLE INFO

Article history:
Received 25 March 2010
Received in revised form 31 May 2010
Accepted 6 June 2010
Available online 23 June 2010

Keywords:
Potentiostatic deposition
Surfactant
Cobalt hydroxide
Specific capacitance
Supercapacitor

ABSTRACT

A N-methylpyrrolidone (NMP) assisted electrochemical deposition route has been developed to realize the synthesis of a dense α-$Co(OH)_2$ layered structure, which is composed of nanosheets, each with a thickness of 10 nm. The capacitive characteristics of the as-obtained α-$Co(OH)_2$ are investigated by means of cyclic voltammetry (CV), charge/discharge characterization, and electrochemical impedance spectroscopy (EIS), in 1 M KOH electrolyte. The results indicate that α-$Co(OH)_2$ prepared in the presence of 20 vol.% NMP has denser and thin layered structure which promotes an increased surface area and a shortened ion diffusion path. The as-prepared α-$Co(OH)_2$ shows better electrochemical performance with specific capacitance of 651 $F g^{-1}$ in a potential range of −0.1 to 0.45 V. These findings suggest that the surfactant-assisted electrochemical deposition is a promising process for building densely packed material systems with enhanced properties, for application in supercapacitors.

1. Introduction

Electrochemical capacitors, also known as supercapacitors, are attracting much attention for energy storage applications. They are found to be attractive because of their higher specific power and longer cycle-life, and also lower energy loss compared with batteries, compressed air and other storage devices. The beneficial properties have made supercapacitors very popular in many applications, especially for mobile electronic devices and electric vehicles [1–3].

Supercapacitors can be categorized into two main types based on their charge-storage mechanisms. They are (i) electrochemical double-layer capacitors (EDLCs), in which charges are stored in the form of an electrical double-layer capacitance, and (ii) pseudo-capacitors, in which Faradic reactions are involved. Electrochemical double-layer capacitors generally have low capacitance, since their charge storage is mainly limited by the available active surface area. In view of this, researchers have focused on increasing the active surface area and have been exploring charge-storage mechanisms at the electrochemical interface. The study of charge storage and ion desolvation behaviour in subnanometer porosity has shown that the matching of active material pore size with electrolyte ion size can help in increasing the capacitance [2,4]. Nevertheless, the capacitance obtained is still considered low at about 100–300 $F g^{-1}$ in aqueous solution [2]. On the other hand, pseudo-capacitors, also called redox-capacitors, have shown higher capacitances due to the presence of Faradic reactions. $RuO_2 \cdot xH_2O$, for example, delivers a capacitance as high as 1300 $F g^{-1}$ [1–3] and stimulated the initial interest in this class of materials. It should be noted, however, that the high cost of this material has directed the research interest to other inexpensive electrode materials with similar good capacitance performance, such as conducting polymers, and other transition metal oxides and nitrides.

Among the new materials, cobalt hydroxide materials have emerged due to their layered structure with a large interlayer spacing [5], which promises high surface area as well as a fast ion insertion/desertion rate. Moreover, their high theoretical specific capacitances and the possibility of enhanced performance through different preparative methods [1–3] have further made them very competitive supercapacitor electrode materials. Nevertheless, there are not many reports of the effect of microstructure modification on the capacitive behaviour of pure cobalt hydroxide [6]. It is noted that, charges are stored in a pseudo-capacitor through surface or near-surface faradic reactions. As a result, it is not surprising that crystal structures, grain size and surface morphologies of electrode materials will strongly affect their capacitance performances [1–3]. To date, various strategies have been taken to synthesize material with high conductivity, high specific surface area and crystal structures or morphologies that favour electrochemical reactions [2,3,7–10]. A flexible nanoflake film of porous

* Corresponding author at: School of Materials Science and Engineering, Nanyang Technological University, Singapore 639798, Singapore. Tel.: +65 67906214; fax: +65 67909081.
E-mail address: asjma@ntu.edu.sg (J. Ma).

0378-7753/$ – see front matter © 2010 Elsevier B.V. All rights reserved.
doi:10.1016/j.jpowsour.2010.06.042

cobalt hydroxide was deposited by galvanostatic electrodeposition on a lightweight and inexpensive stainless-steel mesh and showed a high capacitance of 609 F g^{-1} [6]. Modifications on the microstructure of α-cobalt hydroxide have also been carried out and result in an increment of capacitance [9,11], recently α-cobalt hydroxide nanoflakes are potentiostatically deposited and reports a highest capacitance of 840 F g^{-1} with a potential window of 0.4 V only [8]. As a result, the present work aims to investigate the application of N-methylpyrrolidone (NMP) surfactant-assisted synthesis to the development of various densely packed porous structures, which later can be applied to all hybrid material systems that are based on cobalt hydroxide.

2. Experimental

Analytical grade $Co(NO_3)_2{\cdot}6H_2O$, N-methylpyrrolidone (NMP) and 1 M KOH, as well as stainless-steel (size 1 cm × 1 cm × 0.9 mm), were purchased from Sigma–Aldrich, Singapore. The stainless-steel (SS) plates were polished with emery paper to a rough finish and then washed with ethanol and distilled water before being dried in an oven. A three-electrode electrochemical cell was assembled for electrochemical deposition experiments; it consisted of a platinum foil (2 cm × 2 cm), counter electrode, an Ag|AgCl (saturated KCl solution) reference electrode, and an SS working electrode. The electrolyte solutions for $Co(OH)_2$ deposition were prepared by adding various amounts of NMP, namely, 0, 10, 20 and 30 vol.%, to 0.1 M $Co(NO_3)_2$. The potential of electrochemical deposition was fixed at −1.0 V vs. Ag|AgCl electrode, and the total charge passed through on the cathode was controlled as around 1.0 *C*. The deposition of α-cobalt hydroxide on the SS surface can be expressed by the following reactions [12]:

$$NO_3^- + 7H_2O + 8e^- \rightarrow NH_4^+ + 10OH^- \quad (1)$$

$$Co^{2+} + 2OH^- \rightarrow Co(OH)_2 \quad (2)$$

Both sides of the SS were coated with cobalt hydroxides. The resulting films were then carefully washed with distilled water and dried in air at 60 °C for one day. The weights of the deposits were measured by means of a micro-balance (Mettler Toledo, MT5) with an accuracy of 0.01 mg. The weights of all deposited films were around 0.74 mg.

The surface morphologies of all deposits were investigated via field emission scanning electron microscopy (FESEM, JOEL, JSM-6340F). X-ray diffraction spectra were obtained with an X-ray diffractometer (XRD, RIGAKU, R1NT2100) that used Cu Kα radiation (λ = 1.5406 Å) operating at 40 kV and 30 mA. Data from a Fourier transform infrared spectrometer (FTIR) were collected by means of a PerkinElmer Spectrum GX system. All electrochemical depositions and characterizations of cobalt hydroxide were performed with an AUTOLAB® machine (Eco Chemie, PGSTAT 30). Capacitance characterization was conducted in 1 M KOH electrolyte solution.

3. Results and discussion

The X-ray diffraction (XRD) pattern of the as-obtained $Co(OH)_2$ nanostructure is presented in Fig. 1. The characteristic peaks at 10.46°, 22.58°, 33.74°, 38.14° and 59.08° are attributed to α-$Co(OH)_2$. The peaks marked with an asterisk (*) are assigned to the characteristic peaks of the SS substrate. The FTIR spectrum of the as-obtained α-$Co(OH)_2$ in the presence of 20 vol.% NMP is given in Fig. 2, which is noted to be similar to that of pure α-$Co(OH)_2$. Characteristic peaks at 3488 and 1651 cm^{-1} correspond to the O–H stretching vibrations of interlayer water and free water molecules, respectively. The peak around 1347 cm^{-1} is the characteristic absorption peak of intercalated nitrate. The absorption peaks around 630 and 523 cm^{-1} are assigned to the δ(Co–O–H) and

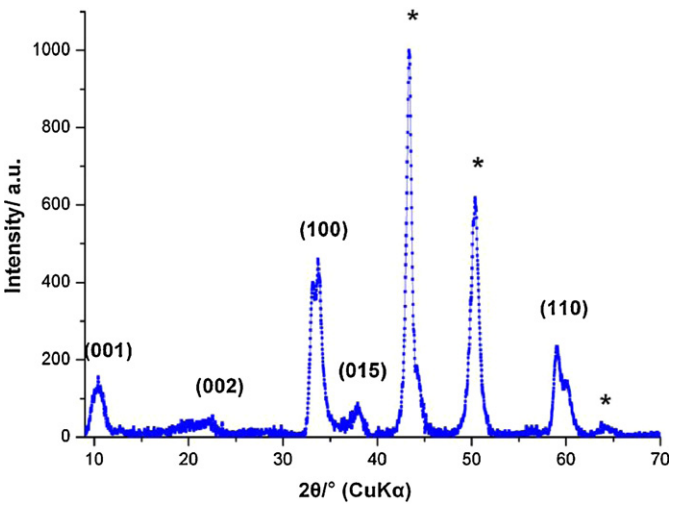

Fig. 1. XRD pattern of as-obtained α-$Co(OH)_2$.

ν(Co–O) stretching vibrations [13,14]. It is noticed that, for cobalt hydroxide (20 vol.% NMP), a distinct absorption peak at 1695 cm^{-1}, which is assigned to C=O stretching in NMP is not observed. These results indicate that the cobalt oxides possess high purity and are in hydrous form with plenty of structure water and NO_3^- ions intercalated.

Field emission scanning electron microscopy images of α-$Co(OH)_2$ deposited under different NMP concentrations are shown in Fig. 3a–f. A characteristic layered structure is observed for all cobalt hydroxide films, in which channels and pores are formed by randomly aligned α-$Co(OH)_2$ nanosheets. A nanostructure with different interlayer distances is observed when different amounts of NMP are added to the deposition electrolytes. The densest structure of cobalt hydroxide is obtained in the presence of 20 vol.% NMP (Fig. 3c). The layer thickness of cobalt hydroxide synthesized in presence of 20 vol.% NMP is about 10 nm (Fig. 3e), which is slightly smaller than that of pure cobalt hydroxide (around 12 nm) (Fig. 3f). Furthermore, some layers of cobalt hydroxide synthesized in the presence of NMP contain several sub-layers, that is only few nanometers thick. From its layer thickness and interlayer distance, it is expected that the nanostructure induced by 20 vol.% NMP will have a high specific surface area and a shorter diffusion path, which

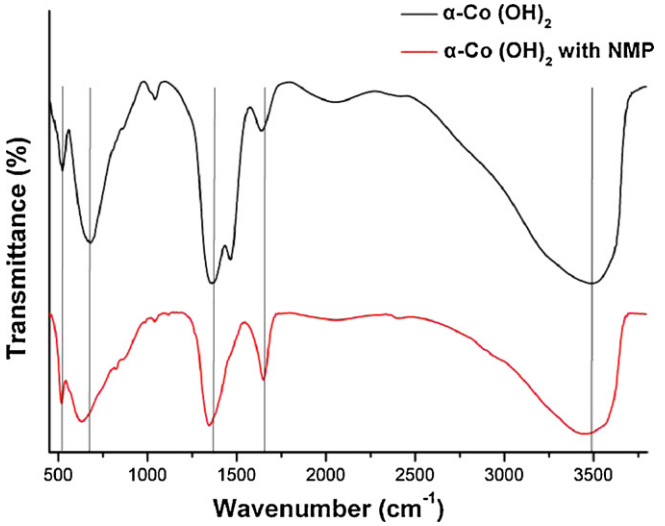

Fig. 2. FTIR spectrum of α-cobalt hydroxide and α-$Co(OH)_2$ prepared under 20 vol.% NMP concentration.

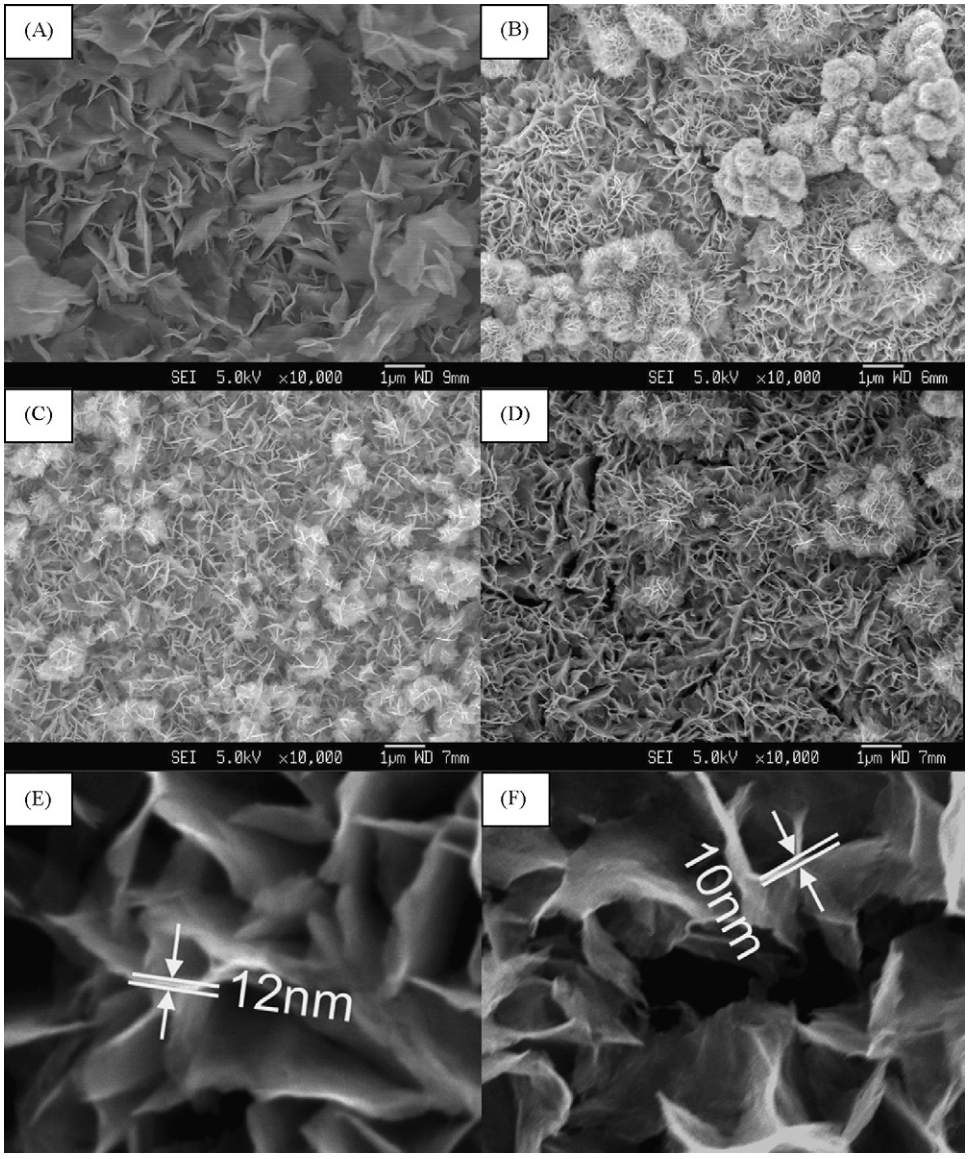

Fig. 3. FESEM images of α-cobalt hydroxides: (a) $Co(OH)_2$, (b) Co10 vol.% NMP hydroxides, (c) Co20 vol.% NMP hydroxides, (d) Co30 vol.% NMP hydroxides, (e) layer thickness of $Co(OH)_2$, and (f) layer thickness of Co20 vol.% NMP hydroxides.

hence provides a structural foundation for a higher specific capacitance [15].

3.1. Electrochemical characterizations

The electrochemical capacitor properties of all forms of as-deposited $Co(OH)_2$ are characterized by cyclic voltammetry (CV) and galvanic charge–discharge characterizations in 1 M KOH aqueous solution. Fig. 4a shows the CV curves of all $Co(OH)_2$ films at a scan rate of $5\,mV\,s^{-1}$, in the potential range of −0.1 to 0.45 V. This potential range is determined by the intrinsic properties of the cobalt hydroxide. Experiments show that when the voltage is higher than 0.45 V, oxygen evolution occurs, whereas when it is lower than −0.1 V, no redox chemical reaction occurs. As shown in Fig. 4a, a pair of reversible redox peaks are visible in the voltage ranges from −0.05 to 0.05, and 0.05 to 0.15 V. For cobalt hydroxides, this surface faradic reaction can be expressed as [16]:

$$Co(OH)_2 + OH^{-1} \leftrightarrow CoOOH + H_2O + e^- \quad (3)$$

The obvious reversible redox peaks and the non-rectangular shape of CV curves indicate that the measured capacitances of $Co(OH)_2$ arise mainly from pseudo-capacitance. The redox current is highest for $Co(OH)_2$ synthesized in the presence of 20 vol.% NMP, and this suggests that its specific capacitance is highest among all the cobalt hydroxides examined in the present work. The discharge curves of deposited $Co(OH)_2$ electrodes in a 1 M KOH electrolyte at $2\,A\,g^{-1}$ in the potential range between −0.1 and 0.45 V are presented in Fig. 4b. The shape of the discharge curve shows the characteristic of pseudo-capacitance, which is directly related to the redox peaks in the CV curves. Their specific capacitances can be calculated from the discharge curve according to following relationship [5]:

$$C_m = \frac{C}{m} = \frac{I \times \Delta t}{\Delta V \times m} \quad (4)$$

where C_m ($F\,g^{-1}$) is the specific capacitance, I (A) is the discharge current, t (s) is the discharging time, V is the discharge potential, and m (g) is the mass of active material within the electrode. The specific capacitances are 473, 571, 651 and $473\,F\,g^{-1}$ for $Co(OH)_2$ synthesized with 0, 10, 20 and 30 vol.% NMP in the electrolyte, respectively. A marked enhancement of capacitance is observed for $Co(OH)_2$ prepared with 20 vol.% NMP in electrolyte. This is

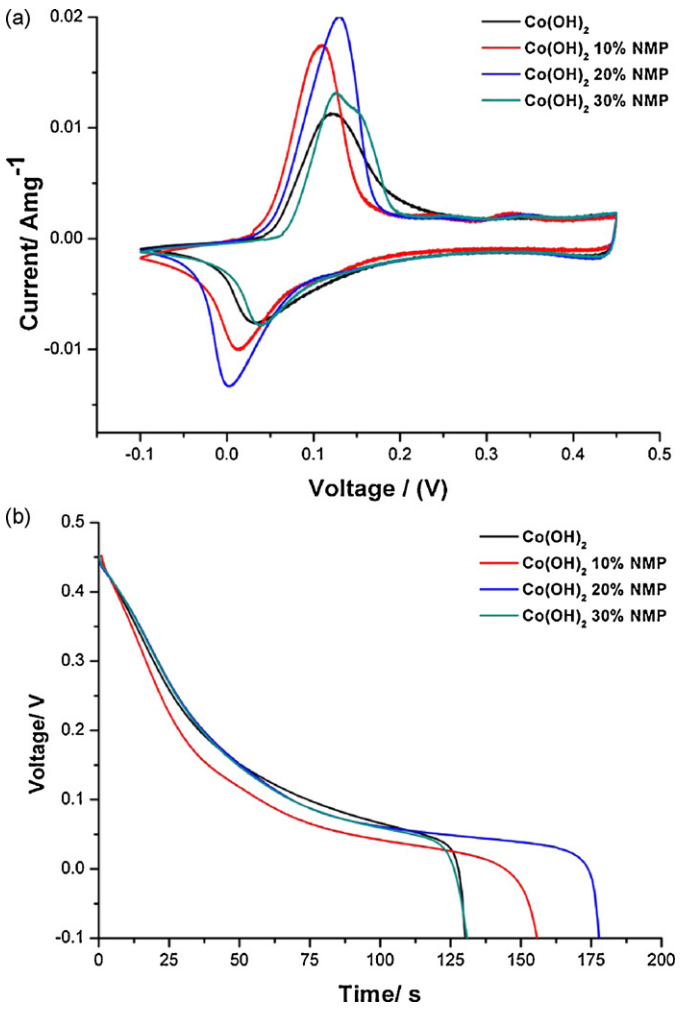

Fig. 4. (a) CV curves of $Co(OH)_2$ films at 5 mV s^{-1} and (b) discharge curves of $Co(OH)_2$ films at 2 A g^{-1}.

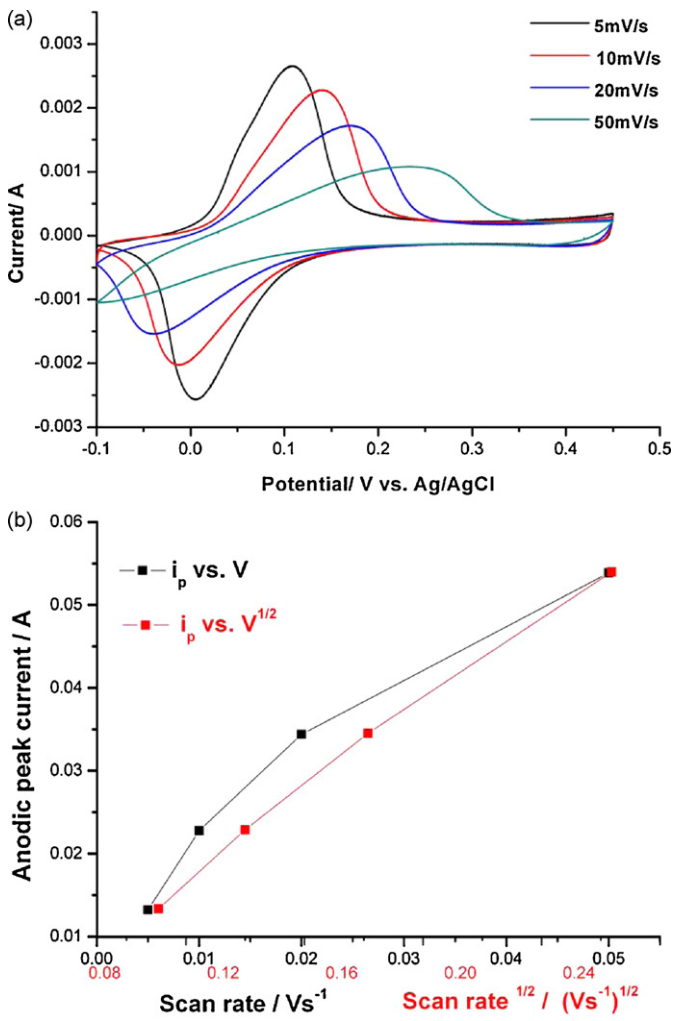

Fig. 5. (a) Cyclic volammograms of $Co(OH)_2$ (20 vol.% NMP) at scan rate of 5, 10, 20, and 50 mV s^{-1}, respectively and (b) i_p vs. $V^{1/2}$ and i_p vs. V plots of $Co(OH)_2$ (20 vol.% NMP).

attributed to its denser and thinner nano-scale microstructure compared with other cobalt hydroxides. The denser and thinner microstructure provides more electrode|electrolyte interfaces and shorter diffusion path for ions, and therefore promotes the electrochemical reactions.

The electrochemical capacitance behaviour of $Co(OH)_2$ (20 vol.% NMP) was further investigated and the results are shown in Fig. 5a, where cyclic voltammograms of $Co(OH)_2$ (20 vol.% NMP) are plotted at different scan rates within the potential range of −0.1 to 0.45 V. The specific capacitance values are calculated to be 604, 572, 527 and 454 F g^{-1} corresponding to a scan rate of 5, 10, 20 and 50 mV s^{-1}, respectively. The data indicates that $Co(OH)_2$ (20 vol.% NMP) has a good rate capability at high current density, a feature that is very important for practical supercapacitor applications.

To study further the CV characteristics of $Co(OH)_2$ (20 vol.% NMP), the anodic peak current i_p vs. V (voltage scan rate), and i_p vs. $V^{1/2}$, are plotted in Fig. 5b. In an absorption process, i_p vs. V is expected to give a linear relationship, irrespective of scan rate [13]. On the other hand, for semi-infinite diffusion-controlled cyclic voltammetry in liquid electrolytes, i_p vs. $V^{1/2}$ is expected to give a linear relationship [13]. It can be seen from Fig. 5 that, i_p vs. V (black line) shows a non-linear relationship, whereas i_p vs. $V^{1/2}$ (red line) shows a reasonably linear plot. Therefore, it is suggested that the redox reaction of the present cobalt hydroxide is diffusion-limited, i.e., a finding that is in agreement with other reports [13].

The cycling stability of cobalt hydroxide prepared in the presence of 20 vol.% NMP is presented in Fig. 6. Electrode was tested at 50 mV s^{-1} for over 500 cycles in the potential range of −0.1 to 0.45 V. Capacitance is observed to decrease slowly with increas-

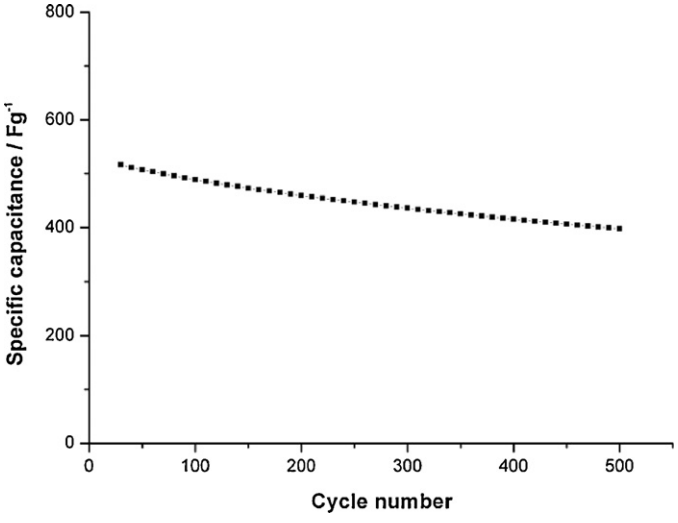

Fig. 6. Cycle-life data of cobalt hydroxide prepared in the presence of 20 vol.% NMP.

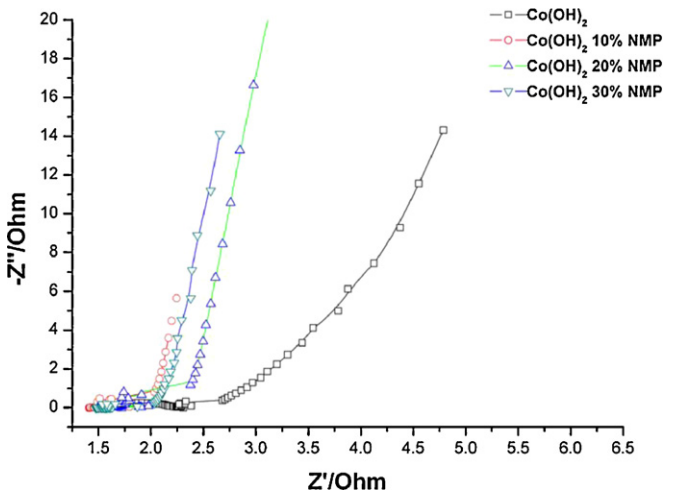

Fig. 7. Nyquist plot of α-$Co(OH)_2$ prepared at different NMP concentrations.

ing cycles and fading is more severe in the first 200 cycles. After 500 cycles, 76% of initial capacitance remains. The fading of capacitance may originate from the slow oxidation of $Co(OH)_2$ to CoOOH owing to the CO^{3+} is more stable than Co^{2+} under alkali environment [17], and some particles exfoliated from thin film during long time cycling may be another reason.

The charge and ion transfer characteristics of all as-obtained $Co(OH)_2$ films are further investigated by using electrochemical impedance spectroscopy (EIS) operating at 0.1 V. The well-known Nyquist diagram, which represents the imaginary part vs. the real part of impedance, is presented shown in Fig. 7. The plots are composed of approximate semi-circles at high frequencies and a slope along the imaginary axis (Z'') at low frequencies. The semi-circle is related to Faradaic reactions and its diameter represents the interfacial charge-transfer resistance (usually termed as Faradaic resistance). The slope is related to the diffusion resistance of the electrolyte in the electrode pores and proton diffusion in the host materials. In Fig. 7, the diameters of the semi-circles of $Co(OH)_2$ prepared with NMP in the electrolyte are smaller than those for material without NMP. The shapes of all four curves are similar, but the slope of the straight line at low frequency for $Co(OH)_2$ prepared with NMP is steeper than that for $Co(OH)_2$ prepared without NMP. The results show that $Co(OH)_2$ samples prepared with NMP surfactant have lower reaction and diffusion resistances. The result also confirms that morphology has a significant effect on electrochemical capacitance.

3.2. Effect of NMP in layered structure synthesis

It has been shown in Fig. 3 that the microstructure of $Co(OH)_2$ changes after certain amount of NMP is added to the deposition solution. The reason may be attributed to the high polarity and dispersity of NMP surfactant in water that results in the formation of a complex surfactant/electrolyte system which provides smaller nucleation centres for $Co(OH)_2$ deposition. During the deposition, Co^{2+} first reacts with OH^- to form short-lived $Co(OH)_2$ dimers. These dimers in a NMP–water system may form a large number of microemulsions which later control the nucleation and growth of the inorganic precipitates [16]. It is also noted that the size of the microemulsion is controlled by the composition of solution [18–20]. In the present study, by controlling the concentration of NMP in the precursor solution, different sizes of nucleation centres are considered to be affected. As a result, the morphology of $Co(OH)_2$ is found to vary with the concentration of NMP in the pre-deposition electrolyte.

4. Conclusions

In conclusion, a simple N-methylpyrrolidone (NMP) surfactant-assisted electrochemical route has been developed to modify the packing density of layered Co $(OH)_2$. It is found that the surface morphology of the cobalt hydroxide can be modified simply by adjusting the amount of NMP concentration in the electrolyte solution. The resulting morphology shows much narrower interlayer spacing after NMP addition, which can provide more active sites for electrochemical reactions. A 37% increment in capacitance is noted when 20 vol.% NMP surfactant is added to the electrolyte solution. The result confirms that microstructure plays a very important role in the property enhancement of the supercapacitor, and 20 vol.% NMP addition produces the most densely packed layered $Co(OH)_2$ in the present investigation.

References

[1] A.S. Arico, P. Bruce, B. Scrosati, J.M. Tarascon, W. Van Schalkwijk, Nat. Mater. 4 (2005) 366–377.
[2] P. Simon, Y. Gogotsi, Nat. Mater. 7 (2008) 845–854.
[3] E.S.S.F.a.T.A. B.E. Conway, Kluwer, New York (1999).
[4] C. John, L. Celine, T. Pierre-Louis, S. Patrice, G. Yury, Angew. Chem. Int. Ed. 47 (2008) 3392–3395.
[5] R.S.J.A.P.V. Kamath, J. Mater. Chem. 9 (1999) 961.
[6] J.Z.W.S.L. Chou, H.K. Liu, S.X. Dou, J. Electrochem. Soc. 155 (2008) A926.
[7] L.H. Su, X.G. Zhang, C.H. Mi, B. Gao, Y. Liu, Phys. Chem. Chem. Phys. 11 (2009) 2195–2202.
[8] V. Gupta, S. Gupta, N. Miura, J. Power Sources 177 (2008) 685–689.
[9] W.J. Zhou, J. Zhang, T. Xue, D.D. Zhao, H.L. Li, J. Mater. Chem. 18 (2008) 905–910.
[10] D. Choi, G.E. Blomgren, P.N. Kumta, Adv. Mater. 18 (2006) 1178–1182.
[11] I.G. Casella, M. Gatta, J. Electroanal. Chem. 534 (2002) 31–38.
[12] X.F. Wang, Z. You, D.B. Ruan, Chin. J. Chem. 24 (2006) 1126–1132.
[13] Z.A. Hu, Y.L. Xie, Y.X. Wang, L.J. Xie, G.R. Fu, X.Q. Jin, Z.Y. Zhang, Y.Y. Yang, H.Y. Wu, J. Phys. Chem. C 113 (2009) 12502–12508.
[14] Z.P. Xu, H.C. Zeng, Chem. Mater. 11 (1998) 67–74.
[15] W.G. Pell, B.E. Conway, J. Electroanal. Chem. 500 (2001) 121–133.
[16] B. Francesca, C. Antonio, C. Umberto, N. Morena, P. Tamara, Eur. J. Inorg. Chem. 2009 (2009) 2603–2611.
[17] Y.-Y. Liang, H.-L. Li, X.-G. Zhang, Mater. Sci. Eng. A 473 (2008) 317–322.
[18] P. Brochette, C. Petit, M.P. Pileni, J. Phys. Chem. 92 (1988) 3505–3511.
[19] M. Zulauf, H.F. Eicke, J. Phys. Chem. 83 (1979) 480–486.
[20] M.P. Pileni, Langmuir 17 (2001) 7476–7486.